JOURNAL OF SOLID STATE CHEMISTRY 73, 140–150 (1988)

Dependence of the Structure and Electronic State of $SrFeO_x$ ($2.5 \leq x \leq 3$) on Composition and Temperature

M. TAKANO,* T. OKITA, N. NAKAYAMA, AND Y. BANDO

Institute for Chemical Research, Kyoto University, Uji, Kyoto-fu, 611, Japan

Y. TAKEDA AND O. YAMAMOTO

Department of Chemistry, Faculty of Engineering, Mie University, Tsu, Mie-ken, 514, Japan

AND J. B. GOODENOUGH†

Inorganic Chemistry Laboratory, South Parks Road, Oxford OX1 3QR, England

Received June 30, 1986; in revised form June 22, 1987

The system $SrFeO_x$, $2.5 \leq x \leq 3$, forms a continuous solid solution at temperatures $T \geq T_t(x)$, but a series of discrete ordered-vacancy phases $SrFeO_{3-(1/n)}$ ($n = \infty$, 8, 4, 2) below temperatures $T_t(n = 8) = 523$ K, $T_t(n = 4) = 598$ K, and $T_t(n = 2) = 1103$ K. The most probable vacancy-ordering schemes for $Sr_8Fe_8O_{23}$ ($n = 8$) and $Sr_4Fe_4O_{11}$ ($n = 4$) are proposed. Formation of fivefold-coordinated iron sites on either side of an oxygen vacancy is characteristic of both phases, which contrasts with $Sr_2Fe_2O_5$ ($n = 2$) where four-coordinated sites coexist with six-coordinated sites. The high-spin $Fe^{4+}(t_{2}^{3}\sigma^{*1})$ configuration of $SrFeO_3$ ($n = \infty$) evolves as follows: (a) for $x \approx 3$, random vacancies trap Fe^{3+} ions at five-coordinated sites; (b) for $n = 8$, Fe^{4+} ions remain high spin, a localized-electron ^5E_g configuration giving rise to a cooperative Jahn–Teller distortion with $c/a \leq 1$ and a $[220]_{n8}$ unique axis imposed by structural symmetry; fast $Fe^{3+} + Fe^{4+} = Fe^{4+} + Fe^{3+}$ electron transfer occurs parallel to this axis at room temperature, but Fe^{3+} ions are ordered at five-coordinated sites at 4 K; (c) for $n = 4$, the octahedral-site Fe^{4+} ions have a low-spin t_2^4 configuration with four near-neighbor Fe^{3+} ions in five-coordinated sites not making an Fe^{3+}–O–Fe^{4+}–O–Fe^{3+} linear chain as in $n = 8$. Oxygen-vacancy hopping times $\tau_h \geq 10^{-8}$ sec persist for 200 K above T_t in $n = 2$, and short-range ordering in this temperature interval is inferred. For $n = 8$ and $n = 4$, motional narrowing to a single Mössbauer peak occurs within tens of degrees above T_t, and this narrowing is assumed to reflect rapid electron hopping in a mixed-valence state; this electronic motion masks any line narrowing due to oxygen-vacancy mobility in these phases.

Introduction

Of the several oxides containing iron in the unusual valence state Fe^{4+}, the cubic

* To whom correspondence should be addressed.

† Present address: Center for Materials Science and Engineering ETC5160, University of Texas at Austin, Austin, Texas 78712-1084.

0022-4596/88 $3.00

perovskite $SrFeO_3$ is perhaps the most interesting for a study of the effects of oxygen deficiency on the electronic and structural properties (*1, 2*).

Stoichiometric $SrFeO_3$ retains the ideal cubic perovskite structure down to at least 4 K. The octahedral-site Fe^{4+} ions are in a high-spin $t_2^3\sigma^{*1}$ configuration, where the orbitally twofold-degenerate, narrow σ^* band of e-orbital parentage is one-quarter filled and therefore imparts a metallic conductivity even though the correlation energies split the majority-spin band from the minority-spin band. Retention of cubic symmetry to low temperatures shows that the electrons of e-orbital parentage induce no cooperative Jahn–Teller distortion, neither the $LaMnO_3$-type (*3*) characteristic of localized e electrons nor the $CaFeO_3$-type disproportionation reaction $2Fe^{4+}(t_2^3\sigma^{*1}) \rightarrow Fe^{(4-\delta)+}(t_2^3\sigma^{*1+\delta}) + Fe^{(4+\delta)+}(t_2^3\sigma^{*1-\delta})$ characteristic of narrow-band electrons (*4, 5*). In addition, there is evidence (*6*) that $SrFeO_3$ may sit near the threshold of a crossover from the high-spin to the low-spin state.

The preparation and characterization of oxygen-deficient compositions $SrFeO_{3-x}$ have been studied previously by several groups (*7–11*), but a more systematic study (*12*) has established the existence of the serial phases $SrFeO_{3-(1/n)}$. In this series, $n = \infty$, 8, 4, and 2 correspond to $SrFeO_3$, $SrFeO_{2.875}$ ($Sr_8Fe_8O_{23}$), $SrFeO_{2.75}$ ($Sr_4Fe_4O_{11}$), and $SrFeO_{2.5}$ ($Sr_2Fe_2O_5$). These are referred to hereinafter as phases $n\infty$, $n8$, $n4$, and $n2$. This latter study also found that above a first-order transition temperature T_t, which is composition-dependent, the oxygen vacancies are disordered in a cubic phase over the whole composition range from $SrFeO_{2.5}$ to $SrFeO_3$. The measured transition temperatures are T_t = 523, 598, and 1103 K for n = 8, 4, and 2, respectively. The transition for the $n2$ phase $Sr_2Fe_2O_5$ has been reported previously (*8, 9, 13*).

In this paper arguments are given for the most probable vacancy ordering in phases $n8$ and $n4$ below T_t, and the implications of this ordering for the 3*d*-electron states at the Fe atoms are discussed. Finally, high-temperature ($>T_t$) Mössbauer spectra are reported; these measurements probe the 3*d*-electron states in the cubic, disordered phases.

Experimental

Samples were prepared by mixing $SrCO_3$ and α-Fe_2O_3 (99.99% purity from Nakarai Chemicals, Ltd.) in a 2 : 1 molar ratio and heating in air at 1273 K for 24 hr. The products were ground, pressed into disks, and heated again in air at 1573 K for 12 hr. Subsequent annealing was carried out at various temperatures between 523 and 1673 K in a 1-atm stream of N_2 (99.99% pure), in air, or under 1–500 atm of O_2. The annealing time ranged from 24 to 300 hr, depending on the temperature. To prevent oxidation on cooling, samples annealed in N_2, air, or 1 atm of O_2 were quenched from the annealing temperature in liquid N_2. Samples annealed under oxygen pressure were cooled rapidly by immersing the stellite autoclave in water. By this method, we were able to prepare samples covering a composition range $2.50 \leq x \leq 2.97$.

The oxygen content was determined by two independent methods: chemical analysis and thermogravimetry. Chemical analysis was done by monitoring the oxidation of Fe^{2+} to Fe^{3+} in a standard solution by iron of a higher oxidation state from the sample (*12*). Thermogravimetric (TG) analysis was done with a Rigaku DTA-6 TG-4 apparatus: the weight loss on heating a sample to 1623 K in a 1-atm N_2 stream where $SrFeO_{2.50}$ is stabilized was measured. The two types of measurement gave good agreement with each other with $|x_{\text{chem. anal.}} - x_{\text{TG}}| \leq 0.03$. The compositions studied are represented by values averaged over the two independent measurements.

X-ray diffractograms were obtained with both monochromated Cu$K\alpha$ and Cu$K\beta$ radiation on a Rigaku RU-200 diffractometer, and order–disorder phase transitions were determined by differential thermal analysis (DTA). Electron diffraction measurements were made with a JEM 100CX on Sr $FeO_{2.97}$, $SrFeO_{2.86}$, and $SrFeO_{2.73}$. These measurements gave microscopic evidence supporting the X-ray data analysis. However, a prolonged electron-beam irradiation for the purpose of obtaining a high-resolution image was found to result in a structural change due to a loss of oxygen.

The Mössbauer spectra obtained at 295 and 4 K showed that, in either the paramagnetic or antiferromagnetic states, the samples $SrFeO_{2.97}$, $SrFeO_{2.86}$, $SrFeO_{2.73}$, and $SrFeO_{2.68}$ gave characteristic spectra, whereas other compositions gave spectra indicative of a two-phase mixture.

The phase diagram resulting from these studies has been published (*12*).

Vacancy Ordering

X-ray diffraction (XRD) and electron diffraction (ED) measurements (*12*) have shown that the unit cells of the room temperature phases *n*8 and *n*4 are enlarged relative to the parent perovskite cell in a manner characteristic of vacancy ordering. Attempts to determine their ordered structures by means of high-resolution electron microscopic observation and neutron diffraction have met difficulties: an oxygen loss occurred on exposure to a strong electron beam and it was difficult to prepare very homogeneous samples large enough for neutron diffraction. So, we propose the most probable vacancy-ordering schemes below.

The single-phase material nearest to the ideal composition *n*8 that was obtained experimentally was $SrFeO_{2.86}$; it had a tetragonal unit cell with lattice constants a_{n8} = 1.0934 nm and c_{n8} = 0.7705 nm. The extinction rule was $h + k + l = 2n$, indicating a body-centered structure. The single-phase $SrFeO_{2.73}$ obtained experimentally corresponds to the ideal $SrFeO_{2.75}$ phase *n*4; it has an orthorhombic cell with a_{n4} = 1.0972 nm, b_{n4} = 0.7700 nm, and c_{n4} = 0.5471 nm. From the extinction rule for $h + k = 2n$, this structure may be assumed to be base-centered. Furthermore, the cell volumes are approximately $(2\sqrt{2}a_p)^2 \times 2a_p$ and $2\sqrt{2}\,a_p \times 2a_p \times \sqrt{2}a_p$, respectively, for phases *n*8 and *n*4, where $a_p \simeq 0.385$ nm is the lattice constant of the cubic perovskite cell. If these two phases are expressed as $Sr_8Fe_8O_{23}$ and $Sr_4Fe_4O_{11}$, then in each case the unit cell contains two formula units. Following the representation of Tofield *et al.* (*8*), Fig. 1 shows vacancy-ordering

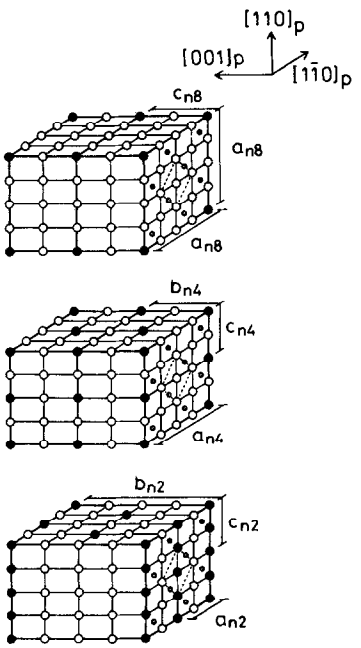

FIG. 1. Proposed body-centered and base-centered vacancy-ordering schemes for phases *n*8 and *n*4, respectively. The well-established scheme for phase *n*2 is also shown for comparison. Open, closed, and dotted small circles indicate O^{2-} ions, vacancies, and Fe ions. *a*, *b*, and *c* with phase-indicating suffixes stand for the unit-cell axes. Dotted lines show the parent perovskite cell.

schemes for phases $n8$ and $n4$ that satisfy these several constraints; it also compares these two schemes with the one well established (*7, 14, 15*) for the phase $n2$.

The orthorhombic cell for phase $n2$ has an approximate volume $\sqrt{2}a_p \times 4a_p \times \sqrt{2}a_p$, which contains four molecules of $Sr_2Fe_2O_5$. In this structure, the oxygen vacancies are ordered into strings along the c_{n2} axis, which is the $[110]_p$ direction of the parent cubic perovskite. The c_{n2} strings of vacancies are located in every other $(001)_p$ plane where they alternate with c_{n2} strings of oxide ions. Thus the Fe^{3+} ions in the $(001)_p$ planes containing oxygen vacancies are each coordinated by four oxide ions; those in the alternate $(001)_p$ planes are six-coordinated in octahedral sites.

In phase $n4$, the model of Fig. 1 shows that the oxygen vacancies are ordered into strings of alternating vacancy and oxide ion along the c_{n4} axis, which is the $[110]_p$ axis. In this case every $(001)_p$ plane contains these c_{n4} strings alternating with three c_{n4} strings of oxide ions. The interplane ordering is such that the phase contains equal numbers of Fe atoms having fivefold and sixfold coordination. This model is the same as that proposed by Tofield *et al.* (*8*) except that their cell is doubled along the c_{n4} axis. Comparison of their Mössbauer-effect (ME) spectrum and ED pattern with ours indicates that their sample contained some of phase $n8$, which has an $a_{n8} = 2c_{n4}$. Gibb (*11*), on the other hand, has inferred a different model on the basis of his ME spectra. In Gibb's model, vacancy-containing $(001)_p$ planes like those found in phase $n2$ are ordered as every fourth $(001)_p$ plane instead of every other. However, this model does not satisfy the diffraction properties reported in Ref. (*12*).

The vacancies in phase $n8$ are further separated from each other; they occupy only the origin and the center of the large unit cell. With this ordering, the unit cell is not truly tetragonal, but orthorhombic, as a result of unequal atomic arrangements along $[110]_{n8}$ and $[\bar{1}10]_{n8}$. In view of a difference of only 0.3% between a_{n4} and $2c_{n4}$ in the more oxygen-deficient phase, it is not unreasonable that lowering of the symmetry from tetragonal to orthorhombic in phase $n8$ was not detected even by a careful X-ray measurement with singlet Cu$K\beta$ radiation (*12*). With the ordering of Fig. 1, a unit cell of phase $n8$ contains 4 iron atoms in fivefold coordination and 12 in sixfold, octahedral coordination.

The diagrammatic representation of Fig. 1 does not indicate the true atomic positions in these phases; in particular the atoms neighboring an oxygen-vacancy relax. If the oxygen atom is removed from a 180° Fe–O–Fe bond, the electrostatic repulsive force between the two cations pushes the Fe atoms apart, and a movement of neighboring anions toward the vacancy also occurs to screen this repulsion. In phase $n2$, for example, the four-coordinated iron atoms occupy more nearly tetrahedral sites than is represented in Fig. 1 while the six-coordinated iron atoms occupy distorted octahedral sites (*14, 15*). The five-coordinated sites in phases $n4$ and $n8$ may occupy sites that approach either trigonal bipyramidal or square pyramidal. Both coordination types have been established for oxides containing trivalent iron such as $BaFe_{12}O_{19}$ (*16*), $FeTiPrO_5$ (*17*), YFe_2O_4 (*18*), and $Sr_4Fe_6O_{13}$ (*19*), but not for oxides containing Fe^{4+} ions (*20*).

Electronic Configurations

The influence of oxygen vacancies on the electronic states of the Fe ions can be probed by Mössbauer measurements, which give complex ME spectra. Figure 2 shows the spectra at 300 and 4 K for $SrFeO_{2.97}$, $SrFeO_{2.86}$, and $SrFeO_{2.73}$; Table I gives the parameter values determined by computer fitting (*12*).

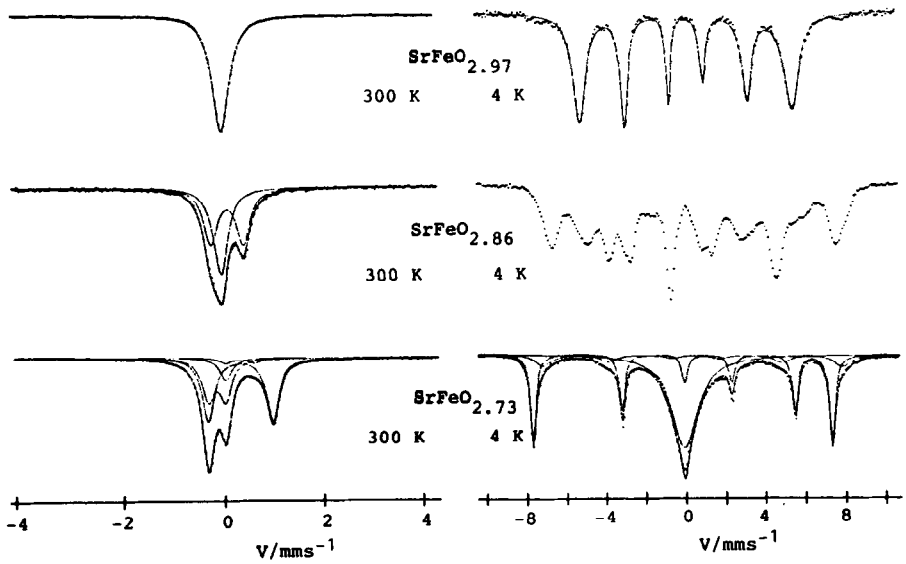

FIG. 2. Mössbauer spectra of $SrFeO_{2.97}$ (phase $n\infty$), $SrFeO_{2.86}$ ($n8$), and $SrFeO_{2.73}$ ($n4$).

$SrFeO_{2.73}$. The spectrum for $SrFeO_{2.73}$, the single-phase material representing $n4$, contains four components. Components 3 and 4 have isomer shifts and hyperfine fields characteristic of an Fe^{3+} ion in its high-spin state. The more important of these, component 3, has a large quadrupolar interaction and can therefore be assigned to high-spin Fe^{3+} ions in five-coordinated sites. Component 4 is characteristic of Fe^{3+} ions in tetrahedral sites; such sites would be created by the presence of excess oxygen vacancies. Components 1 and 2 arise from Fe^{4+} ions in octahedral sites; the more important of these, component 1, has a negative isomer shift and can be assigned to the low-spin (LS) $^3T_{1g}$ state whereas component 2 corresponds to Fe^{4+} in a high-spin (HS) state. We assume that the high-spin Fe^{4+} ions reflect a residual disorder.

TABLE I

MÖSSBAUER DATA FOR PHASES $n\infty$, $n8$, AND $n4$ OF THE $SrFeO_{3-1/n}$ SYSTEM

		300 K				4 K				
$3-1/n$	Component	IS/mm/sec	ΔE/mm/sec	%	Valence	IS/mm/sec	ΔE/mm/sec	Hi/T	Valence	%
2.97	1	0.06	—	94	Fe^{4+}(HS)	0.2	—	33	Fe^{4+}	95
($n\infty$)	2	0.32	—	6	Fe^{3+}	0.4	—	51	Fe^{3+}	5
2.86	1	0.04	—	45	Fe^{4+}(HS)	0.0	—	29	Fe^{4+}	50
($n8$)	2	0.17	0.84	55	$Fe^{3.5+}$	0.4	—	44	Fe^{3+}	30
2.73	1	−0.09	0.34	33	Fe^{4+}(LS)	Very broad absorption				48
	2	0.11	—	9	Fe^{4+}(HS)	centered around ~0 mm s^{-1}				
($n4$)	3	0.37	1.29	53	Fe^{3+}	0.5	−1.29	46	Fe^{3+}	38
	4	0.35	0.58	5	Fe^{3+}	0.4	0.3	47	Fe^{3+}	14

Note. IS, isomer shift vs metallic iron; ΔE, quadrupole splitting= $\frac{1}{2}e^2qQ(1 + \eta^2/3)^{1/2}$; Hi, magnetic hyperfine field; HS, high-spin state; LS, low-spin state.

Computer analysis of the ME spectrum at 4 K indicated that the electric-field-gradient (efg) tensor for component 3 is almost uniaxial with its unique component, eq = V_{zz}, having a negative sign and its unique axis parallel to the spin axis. However, comparison of the parameters for component 3 with the sparse literature values for five-coordinated Fe^{3+}, which are available only for the above-mentioned oxides (*21–24*), failed to provide a conclusive identification of the coordination polyhedron as trigonal bipyramidal vs square pyramidal. From a simple point-charge calculation, it appears that the efg for either of these sites is quite sensitive to the Fe position along the unique axis, which leads to an overlapping scatter in the observed ME spectra. Nevertheless, if the polyhedron is a square pyramid with an Fe^{3+} ion on its fourfold-symmetry axis, the spin axis should be along $[102]_{n4}$, the unique axis in this case. On the other hand, if the polyhedron is a trigonal bipyramid with an Fe^{3+} ion on its threefold-symmetry axis, the efg and spin axes should be parallel to $[\bar{1}02]_{n4}$. The geometry of the ordered phase would appear to favor the latter alternative.

The spin-orbit interaction at an Fe^{4+} : $^3T_{1g}$ state, component 1, gives states with total angular momenta 0, 1, and 2 with the singlet lowest for the positive coupling parameter (*25*). In the magnetically ordered state, this component shows a slightly broadened absorption, which contrasts with the well-defined magnetic pattern for the high-spin state Fe^{4+} ion in $SrFeO_{2.97}$. This finding is consistent with the nonmagnetic, singlet ground state of LS Fe^{4+} ions. The broadening would, in this case, result from a supertransferred hyperfine interaction with neighboring, magnetically ordered Fe^{3+} ions and/or from a small magnetic moment induced by a second-order perturbation. Such a coexistence of nonmagnetic and magnetic iron atoms has been reported previously for $Sr_2FeO_{3.7}$ and $Sr_3Fe_2O_{6.2}$ (*26*); the above interpretation is applicable to these materials also.

$SrFeO_{2.86}$. The ME spectrum for $SrFeO_{2.86}$ has two components of nearly equal intensity at room temperature. The isomer shift of component 1 corresponds to that for a HS Fe^{4+} ion; the isomer shift of component 2 is intermediate between the HS Fe^{4+} and Fe^{3+} state, which suggests fast $Fe^{4+} + Fe^{3+} = Fe^{3+} + Fe^{4+}$ electron transfer relative to 10^{-8} sec. If component 2 were due to charge-compensating Fe^{3+} ions, the intensity ratio of component 1 to component 2 should be 3 : 1.

To relate this finding to the proposed structure of Fig. 1, the atomic arrangements in the two types of $(220)_{n8}$ planes—where the Fe atoms and oxygen vacancies reside—are shown in Fig. 3. Half of the $(220)_{n8}$ planes contain no vacancies; we can

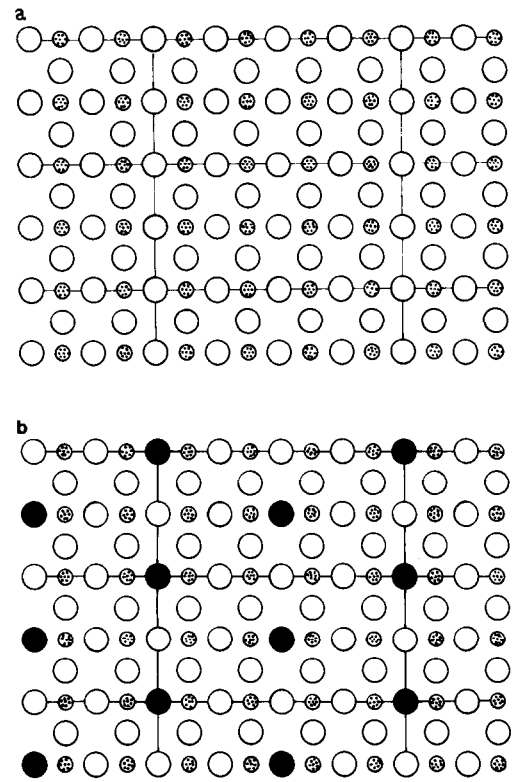

FIG. 3. Atomic arrangements in the (220) planes of phase *n*8 without (a) and with (b) vacancies.

assign the octahedrally coordinated Fe atoms in these planes to be the high-spin Fe^{4+} ions responsible for component 1 in the ME spectrum. The remaining $(220)_{n8}$ planes contain equal concentrations of five-coordinated and six-coordinated iron atoms, and site-preference energies call for ordering of the Fe^{3+} ions into the five-coordinated sites and Fe^{4+} ions into the six-coordinated sites. However, the room temperature ME spectrum indicates fast-electron transfer between Fe^{3+} ions and one-third of the Fe^{4+} ions. Rapid electron exchange between Fe^{3+} and Fe^{4+} ions has been observed previously for the mixed-valent perovskites $Ca_{1-x}La_xFeO_3$ and $Sr_{1-y}La_yFeO_3$ (*1*, *27*). The question of which third of the octahedral-site Fe^{4+} ions participate in the fast-electron transfer remains open, but theoretical considerations favor one-dimensional fast-electron transfer along the $[220]_{n8}$ axes between $(220)_{n8}$ planes and not two-dimensional transfer within $(220)_{n8}$ planes.

The theoretical argument goes as follows: The strongest atomic relaxations must occur within the $(220)_{n8}$ planes containing oxygen vacancies and Fe^{3+} ions. The Fe^{3+} ions facing each other across a vacancy would repel each other, and the four in-plane oxide ions neighboring a vacancy would be displaced toward the vacancy so as to better screen the Fe^{3+} ions from one another and to make the Fe^{3+}-ion site approach a trigonal bipyramid. These atomic displacements create a unique $[220]_{n8}$ axis in which nearly 180° Fe–O–Fe interactions are preserved between alternating $(220)_{n8}$ planes. Within the vacancy-containing $(220)_{n8}$ planes, the octahedral sites are strongly distorted and the Fe–O–Fe bond angles deviate significantly from 180°. Since fast-electron transfer requires a strong σ-bond Fe–O–Fe interaction, which is maximized for a 180° Fe–O–Fe bond angle, it can be anticipated that the strongest Fe–O–Fe interaction is parallel to the $[220]_{n8}$ axis. If this direction is taken to be the z axis, then nearly 180° $Fe^{3+}: d_{z^2}$–$O: p_z$–$Fe^{4+}: d_{z^2}$ interactions occur between five-coordinated and six-coordinated Fe atoms of alternate $(220)_{n8}$ planes that could be strong enough to form a narrow $\sigma^*_{z^2}$ band of d_{z^2}-orbital parentage that is one-quarter filled. Such a solution implies a cooperative, tetragonal ($c/a \leq 1$) Jahn–Teller distortion of the HS $Fe^{4+}: d^4$ octahedral sites with a unique $[220]_{n8}$ axis. Although this is not the normal sign of the localized-electron Jahn–Teller distortion at an octahedral-site HS d^4 configuration, the atomic relaxations in the $(220)_{n8}$ planes containing vacancies would produce an expansion in that plane and thus a stress on the octahedral sites of both $(220)_{n8}$ planes favoring a $c/a < 1$.

The more complex spectrum at 4 K lends support to this model. The hyperfine parameters show a broad distribution with two well-defined population peaks at the values given in Table I. At this temperature, the mobile electrons would be trapped at the five-coordinated sites to give about 25% of the spectrum a peak characteristic of HS Fe^{3+} in a five-coordinated site. The HS Fe^{4+} ions would contribute the remainder with a peak characteristic of the HS Fe^{4+} ions in the $(220)_{n8}$ planes containing no vacancies; the contribution from Fe^{4+} ions in the distorted octahedral sites of a vacancy-containing $(220)_{n8}$ plane could be responsible for the broad background. Such an ordering of Fe^{4+} and Fe^{3+} ions, or at least a slowing of the charge transfer to a $\tau \geq 10^{-8}$ sec, to split the $Fe^{3.5+}$ line in two is to be distinguished from the disproportionation reaction $2\ Fe^{4+} \rightarrow Fe^{(4+\delta)+} + Fe^{(4-\delta)+}$ found (*1*) in $CaFeO_3$, which splits the Fe^{4+}-ion line in two.

$SrFeO_{2.97}$. The room temperature and 4 K spectra of $SrFeO_{2.97}$ are similar to those of stoichiometric $SrFeO_3$ except that a weak additional component coming from Fe^{3+} ions is superposed. The intensity ratio for the Fe^{3+} and Fe^{4+} peaks coincides with the

one expected from simple charge compensation for the given oxygen-vacancy concentrations. The small concentration of vacancies appears to be randomly distributed, and isolated vacancies trap two Fe^{3+} ions.

Summary. Several systematic observations can now be made about the electronic configurations at Fe atoms in the oxygen-deficient $A^{2+}FeO_{3-x}$ perovskites. (1) Fe^{3+} ions tend to be trapped at opposite sides of an oxygen vacancy. (2) Atomic relaxations about the oxygen vacancies narrow the strongly correlated σ^* bands of *e*-orbital parentage so as to introduce localized-electron configurations and thus the possibility of cooperative Jahn–Teller distortions characteristic of a localized d^4 configuration at HS octahedral-site Fe^{4+} ions. (3) The sign of any Jahn–Teller distortion is influenced by internal stresses imposed by atomic relaxations and lattice matching wherever intergrowths of vacancy-free and vacancy-containing planes reflect the vacancy ordering. (4) Any $Fe^{4+} + Fe^{3+} \rightarrow Fe^{3+} + Fe^{4+}$ charge transfer can only occur in those crystallographic directions where Jahn–Teller ordering of a HS d^4 configuration induces overlap of the empty σ-bonding *d*-orbital at the Fe^{4+} ion with the half-filled σ-bonding *d*-orbital at the Fe^{3+} ion. (5) In many Fe^{3+}–O–Fe^{4+} interactions, weaker Fe^{3+}–O covalent bonding strengthens the Fe^{4+}–O bonding on the opposite side of the oxide ion via the "inductive effect." Where an Fe^{4+} ion has two or more Fe^{3+} ion near neighbors that are not collinear, as in phase *n*4, the LS Fe^{4+}-ion state is stabilized; where two Fe^{3+}-ion neighbors are collinear with the Fe^{4+} ion, as in phase *n*8, a HS configuration may be stabilized by a Jahn–Teller ordering at the Fe^{4+} ion; in this case, the Jahn–Teller ordering causes the empty *d* orbital at a HS Fe^{4+} ion to overlap the half-filled σ-bonding *d* orbitals of the two Fe^{3+} ion near neighbors. (6) At room temperature, fast ($\tau_h < 10^{-8}$ sec) electron transfer between Fe^{3+} and Fe^{4+} ions may occur where the Fe–O–Fe bond angle is near 180°.

Additional comment. Single-phase ME spectra and their interpretation have already been reported (*9*). Independent measurements were also made by Gibb (*11*). As mentioned above, Gibb assumed a monophasic compositional range between Sr $FeO_{2.85}$ and $SrFeO_{2.75}$ and an incorrect vacancy-ordering scheme. Consequently his interpretations were quite different.

Disordered Vacancies

DTA and XRD measurements revealed that, above a first-order transition temperature T_t, a single cubic perovskite phase is formed over the whole compositional range $SrFeO_{2.5}$ to $SrFeO_3$ (*12*). It would be interesting to study with electron microscopy (EM) the extent to which the vacancy distribution remains "random" as the vacancy concentration increases. However, EM encounters difficulties associated with compositional changes in a high vaccum at temperatures $T > T_t$. Therefore we chose to follow the evolution of the electronic configurations at the iron atoms with ME spectroscopy since these measurements can be made rather easily under various oxygen partial pressures ($PO_2 < 2 \times 10^5$ Pa) either by flowing mixed gases over samples or by sealing the samples in thin quartz tubes. Through the ME spectra it is also possible to obtain some insights into the structure.

*Phase n*2. Figure 4 shows the ME spectra for phase *n*2 obtained above and below T_t for a powder sample spread on a thin Pt foil. Sample quality was certified not only by checking the reproducibility and reversibility of the spectra on passing through T_t = 1103 K, but also by comparing the spectra for PO_2 at 10^{-2} and 10 Pa. Little difference was detected between spectra taken at different oxygen partial pressures below 1220 K; at higher temperatures, samples under the low PO_2 tended to decompose

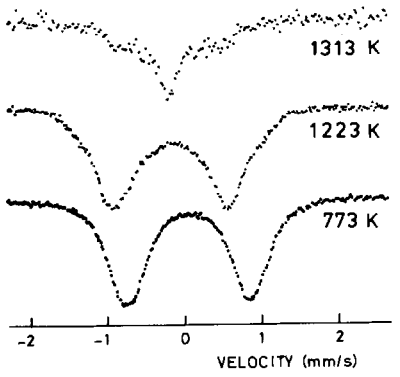

FIG. 4. Mössbauer spectra of $SrFeO_{2.5}$ above and below the transition temperature of 1103 K.

during the period of a prolonged measurement.

The isomer shifts and quadrupole splittings for Fe^{3+} ions in octahedral and tetrahedral sites are almost identical, so the spectrum for the ordered state at 773 K looks like a single quadrupole doublet consisting of slightly broadened peaks, as observed also for $CaFeO_{2.5}$ (*28*). On heating through T_t, the experimental spectrum retains the character of a broadened doublet even up to ca. 1300 K; the splitting at 1273 K is only reduced by about 10% from its value at 773 K. However, broadened peak tails at 1223 K indicate the onset of a collapse of the quadrupole splitting, and at 1313 K the strong influence of motional narrowing is clearly apparent. The motional narrowing indicates hopping of a transient species from site to site in a time $\tau_h < 10^{-8}$ sec. In the absence of sample reduction, the mobile species in this case must be the oxygen vacancies.

Interpretation of these findings remains incomplete. It is clear that on traversing the order–disorder transition temperature T_t, the high-temperature mobility of the oxygen vacancies retains a jump time $\tau_h < 10^{-8}$ sec for nearly 200°C above $T_t \approx 1103$ K and that the majority of the iron atoms remain four- and six-coordinated. However, the ME measurements provide little direct information on the degree of short-range order in that temperature interval. Grenier *et al.* (*10*) have argued for retention of a short-range microdomain structure. Formation of a small concentration of fivefold-coordinated sites in the domain boundaries would not change drastically the ME spectrum on passing from the ordered to the disordered states if the domain size is large enough to suppress the boundary effect. However, even just above T_t our high-temperature XRD measurements failed to detect any diffuse peaks useful for estimating microdomain size, which is to be contrasted with the situation for $SrFe_{1-x}V_xO_{2.5+x}$ where a

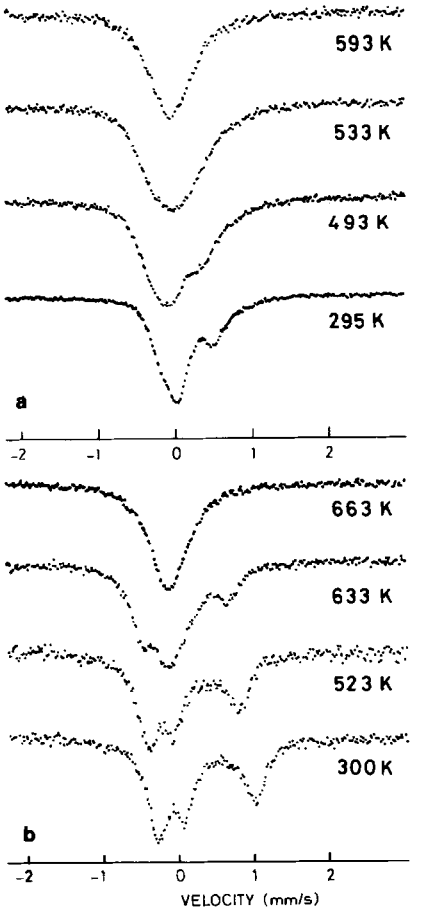

FIG. 5. Mössbauer spectra of $SrFeO_{2.83}$ (a) and $SrFeO_{2.75}$ (b) in the ordered and disordered states.

well-defined microdomain size of 10^3 nm^3 could be detected (*29*). This finding indicates that any microdomains associated with short-range order in phase *n*2 have a smaller size.

Phases n4 and n8. The ME spectra for $SrFeO_{2.83}$ and $SrFeO_{2.75}$ above and below T_t are shown in Fig. 5. The samples were sealed in quartz tubes of 0.7 mm diameter with a wall thickness of 0.1 mm in order to minimize changes in oxygen content during the measurements.

In both samples, a single ME peak characteristic of a time-averaged cubic symmetry was observed at temperatures well above T_t. The collapse to the singlet spectrum occurs gradually with increasing temperature, not suddenly at T_t, for both phases. In $SrFeO_{2.75}$, for example, the peak at about 1 mm/sec coming from the five-fold-coordinated iron persists to a few tens of degrees above the transition temperature T_t = 598 K. This finding indicates the persistence of short-range electronic ordering in addition to short-range vacancy ordering.

Summary. The high-temperature ME data indicate that motional narrowing associated with vacancy disorder is not observed until temperatures are nearly 200°C above T_t and that motional narrowing associated with mixed-valence electron hopping is not observed for tens of degrees above T_t.

Acknowledgment

The authors thank the Japanese Ministry of Education, Science and Culture for their financial support by a grant-in-aid.

References

1. M. TAKANO AND Y. TAKEDA, *Bull. Inst. Chem. Res. Kyoto Univ.* **61,** 406 (1983), and references cited therein.
2. C. GLEITZER AND J. B. GOODENOUGH, "Structure and Bonding," Vol. 61, Chap. 1, Springer-Verlag, Berlin, 1985.
3. J. B. GOODENOUGH, *Phys. Rev.* **100,** 564 (1955).
4. M. TAKANO, N. NAKANISHI, Y. TAKEDA, S. NAKA, AND T. TAKADA, *Mater. Res. Bull.* **12,** 923 (1977).
5. J. B. GOODENOUGH, *J. Solid State Chem.* **12,** 148 (1975).
6. T. TAKEDA, S. KOMURA, AND H. FUJI, *J. Magn. Magn. Mater.* **31–34,** 797 (1983).
7. P. K. GALLAGHER, J. B. MACCHESNEY, AND D. N. E. BUCHANAN, *J. Chem. Phys.* **41,** 2429 (1964); and J. B. MACCHESNEY, R. C. SHERWOOD, AND J. F. POTTER, *J. Chem. Phys.* **43,** 1907 (1965).
8. B. C. TOFIELD, C. GREAVES, AND B. E. F. FENDER, *Mater. Res. Bull.* **10,** 737 (1975); and B. C. Tofield, *React. Solids, 8th Int. Symp.*, p. 253 (1973).
9. M. TAKANO, N. NAKANISHI, Y. TAKEDA, AND T. SHINJO, *in* "Ferrites, Proceedings of the International Conference, 1980, Japan" (H. Watanabe, S. Iida, and M. Sugimoto, Eds.), p. 389, Center for Academic Publication, Japan (1981).
10. N. EA, These Docteur 3^{em} Cycle, Université de Bordeaux 1 (1983); and J.-C. GRENIER, N. EA, M. POUCHARD, AND P. HAGENMULLER, *J. Solid State Chem.* **58,** 243 (1985).
11. T. C. GIBB, *J. Chem. Soc. Dalton Trans.*, 1455 (1985).
12. Y. TAKEDA, K. KANNO, T. TAKADA, O. YAMAMOTO, M. TAKANO, N. NAKAYAMA, AND Y. BANDO, *J. Solid State Chem.* **63,** 237 (1986).
13. S. SHIN, M. YONEMURA, AND H. IKAWA, *Mater. Res. Bull.* **13,** 1017 (1978).
14. C. GREAVES, A. J. JACOBSON, B. C. TOFIELD, AND B. E. F. FENDER, *Acta Crystallogr. Sect. B* **31,** 641 (1975).
15. M. VON-HARDER AND J. K. MÜLLER-BUSCHBAUM, *Z. Anorg. Allg. Chem.* **464,** 169 (1980).
16. X. OBRADORS, A. COOLOMB, M. PERNET, D. SAMARAS, AND J. C. JOUBERT, *J. Solid State Chem.* **56,** 171 (1985).
17. G. BUISSON, *J. Phys. Chem. Solid* **31,** 1171 (1970).
18. N. KATO, I. KAWADA, N. KIMIZUKA, AND T. KATSURA, *Z. Kristallogr.* **141,** 314 (1975).
19. A. YOSHIASA, K. UENO, F. KANAMARU, AND H. HORICUCHI, *Mater. Res. Bull.* **21,** 175 (1986).
20. A. J. JACOBSON, *Acta Crystallogr. Sect. B* **32,** 1087 (1976).
21. R. H. VOGEL AND B. J. EVANS, *J. Appl. Phys.* **49,** 1570 (1978).
22. P. J. SCHURER AND A. H. MORRISH, *Phys. Rev. B* **1,** 951 (1977).
23. M. TANAKA, M. KATO, N. KIMIZUKA, AND K. SHIRATORI, *J. Phys. Soc. Japan* **47,** 1737 (1979).

24. F. KANAMARU, M. SHIMADA, AND M. KOIZUMI, *J. Phys. Chem. Solids* **33,** 1169 (1972).
25. J. B. GOODENOUGH, *in* "Progress in Solid State Chemistry" (H. Reiss, Ed.), Vol. 5, Chap. 4, Pergamon, New York (1971).
26. P. K. GALLAGHER, J. B. MACCHESNEY, AND D. N. E. BUCHANAN, *J. Chem. Phys.* **45,** 2466 (1966).
27. S. KOMORNICKI, L. FOURNES, J.-C. GRENIER, F. MÉNIL, M. POUCHARD, AND P. HAGENMULLER, *Mater. Res. Bull* **16,** 967 (1981).
28. S. GELLER, R. W. GRANT, AND U. GONSER, *in* "Progress in Solid State Chemistry" (H. Reiss, Ed.), Vol. 5, Chap. 1, Pergamon, New York (1971).
29. N. NAKAYAMA, M. TAKANO, S. INAMURA, N. NAKASHISHI, AND K. KOSUGE, *J. Solid State Chem.* **71,** 403 (1987).